Sequencing the Sturtian icehouse

Busfield, M. E.; Le Heron, D. P.

Published in:
Journal of the Geological Society

DOI:
10.1144/jgs2013-067

Publication date:
2014

Citation for published version (APA):
Busfield, M. E., & Le Heron, D. P. (2014). Sequencing the Sturtian icehouse: Dynamic ice behaviour in South Australia. *Journal of the Geological Society*, *171*(3), 443-456. https://doi.org/10.1144/jgs2013-067

Sequencing the Sturtian icehouse: dynamic ice behaviour in South Australia

M.E. BUSFIELD[1]*, D.P. LE HERON[1]

[1]*Department of Earth Sciences, Royal Holloway, University of London, Egham, TW20 0EX, United Kingdom*

**Corresponding author (email: Marie.Busfield.2011@live.rhul.ac.uk)*

Abstract

The Cryogenian record of South Australia houses the type region of the Sturtian glaciation, the oldest of three pan-global icehouse intervals during the Neoproterozoic. Data are presented from previously little described sections at Holowilena Creek, Oladdie Creek and Hillpara Creek in the central and southern Flinders Ranges, where five facies associations are recognized. These are (i) diamictite and conglomerate, (ii) interbedded heterolithics, (iii) hummocky cross-stratified sandstone, (iv) lonestone-bearing siltstone, and (v) ferruginous siltstone and sandstone. The succession reveals significant lateral and vertical facies variation, which is linked to a complex inherited palaeotopography and distance from the sediment source. Repeated stratigraphic occurrences of striated clasts and abundant ice-rafted debris strongly support recurrent glacial influence on sedimentation. The intercalation of gravitationally re-worked diamictites, dropstone-bearing siltstone and dropstone-free siltstone testifies to dynamic sedimentation within a periodically glacially-influenced subaqueous environment. Sequence stratigraphic analysis identifies four glacial advance systems tracts (GAST), separated by three glacial retreat systems tracts (GRST), wherein hummocky cross-stratified sandstones attest to open water conditions. These findings support dynamic ice sheet behaviour in South Australia, and provide clear evidence for repeated intra-Sturtian ice sheet recession.

Introduction

Two Neoproterozoic icehouse intervals have long been recognised in South Australia (Mawson & Sprigg, 1950), namely the older Sturtian and younger Marinoan glaciations, so named after the Sturt Gorge and Marino Rocks of Adelaide's outer suburbs (Preiss et al., 1998). The recognition of broadly age-equivalent deposits worldwide contributed to the development of the snowball Earth hypothesis (Hoffman et al., 1998; Hoffman & Schrag, 2002), wherein two distinct episodes of severe pan-global glaciation enabled ice sheets to extend to low palaeolatitudes, resulting in a supressed hydrological cycle. Recent studies, however, support a considerably more dynamic cryosphere, with fluctuating ice margins, open water areas, and abundant evidence of hydrological activity (e.g. Etienne et al., 2007; Arnaud et al., 2011 and refs therein). Moreover, new age constraints, and their likely error bars, cast doubt on the pan-global synchronicity of these glacial events (e.g. Allen & Etienne, 2008; Condon & Bowring, 2011), and hence their two-fold subdivision as 'Sturtian' or 'Marinoan'. This holds significant bearing on the Neoproterozoic glacial deposits of South Australia, widely considered as the type area of the Sturtian icehouse period (Hoffman & Schrag, 2002).

The Adelaide Fold Belt of South Australia (Figs. 1-2) exposes an extremely thick succession of diamictite, sandstone and siltstone, thought to have accumulated during the Sturtian glaciation. The glacial affinity of these sediments was first proposed by Howchin (1901), arguing in favour of glaciomarine deposition (Howchin, 1908), although correlative sections were subsequently interpreted as terrestrial glacial deposits by Mawson (1941, 1949). Detailed examination of sections in the northern Flinders Ranges and Mount Painter area by Link and Gostin (1981) and Young and Gostin (1988, 1989, 1990, 1991) heralded a return to the glaciomarine hypothesis. The latter studies identify a four-fold stratigraphic subdivision, consisting of two principal diamictite units, each overlain by a succession of siltstones and sandstones, interpreted to record two glacial cycles within the Sturtian interval. The thickness of studied sections varies considerably across the region from a

few hundred metres, to a purported 6000 m in the Yudnamutana Trough (Fig. 2), attributed either to the development of subglacial palaeovalleys, to active extensional tectonics, or a combination of the above (Young & Gostin, 1990, 1991; Preiss, 2000).

Comparatively few detailed sedimentological studies have been conducted on the Sturtian deposits of the central and southern Flinders Ranges. Regional mapping identifies a major fault-bound depocentre in the Barratta Trough (Fig. 2), where Sturtian sediments attain an estimated thickness of 4000 m (Preiss, 1999, and refs therein), thinning to a few hundred metres in adjacent shelf areas (Preiss et al., 1993). Recent work by Le Heron et al. (2011a, b) at Holowilena Creek, in the central Flinders Ranges, records a thick (>800 m) succession of heterogeneous glacigenic strata, with abundant evidence of striated erratic clasts and ice-rafted debris (IRD). Significantly, the occurrence of dropstone-free, hummocky cross-stratified sediments punctuating the succession is interpreted as an interglacial sequence during the Sturtian interval, pointing to major ice sheet fluctuation.

This paper will build upon earlier work by Le Heron et al. (2011a, b) at Holowilena Creek, and present high resolution datasets for correlative sections at Oladdie Creek and Hillpara Creek, approximately 60 km further south and south-east (Fig. 1), previously described only at the reconnaissance level by Binks (1968). These sections enable the facies variability of ice-proximal to more ice-distal settings to be examined, and the influence of pre-existing topographic relief to be tested. A new sedimentary model is presented which frames the development of the diamictite-bearing successions in a glacial sequence stratigraphic context.

Study area and stratigraphy

The studied sedimentary successions belong to the mid Cryogenian Yudnamutana Subgroup, at the base of the Umberatana Group (Fig. 3). In the Adelaide Fold Belt, these sediments rest with angular unconformity upon sandstones and siltstones of the underlying Burra Group (Coats & Preiss, 1987). Stratigraphic nomenclature is highly variable across the region, but typically includes a basal

diamictite-dominated unit, namely the Bolla Bollana Formation to the north, the Pualco Tillite in the central regions, the Appila Tillite further south, or the Sturt Tillite in the type-section of the Adelaide Hills. These pass upwards into more heterogeneous diamictite, sandstone and siltstone facies of the Wilyerpa Formation in the central region, or the Lyndhurst Formation to the north. These deposits are in turn blanketed by the post-glacial Tindelpina Shale Member of the Tapley Hill Formation throughout the Adelaide Fold Belt (Fig. 3). Re-Os dating of the Tindelpina Shale Member provides a minimum age constraint of 643 ± 2.4 Ma for the Yudnamutana Subgroup (Kendall et al., 2006), further corroborated by a U-Pb zircon date of 659 ± 6 Ma derived from a volcaniclastic horizon towards the top of the Wilyerpa Formation (Fanning & Link, 2006).

In places, ironstone facies characterise the lower Yudnamutana Subgroup, ascribed to the Holowilena Ironstone Formation in the study area (Fig. 3), or its correlative the Braemar Ironstone Formation to the east (Forbes, 1989). The Holowilena Ironstone is variously interpreted as overlying the Pualco Tillite, (and equivalent Appila Tillite), or alternatively considered as laterally correlative (Preiss et al. 1993 and refs within). In view of this, we adopt the term 'Holowilena Ironstone' in reference to the distinctly ferruginous facies. The terms 'Pualco Tillite' and 'Wilyerpa Formation' will be adopted to describe the underlying and overlying sedimentary facies, respectively.

The study areas occur within broadly NE-SW trending outcrop belts which span the Parachilna and Orroroo map sheets (Fig. 1; Binks, 1968; Preiss, 1999). The orientation of these outcrops is considered to reflect widespread Willouran to early Sturtian rifting (*c.* 830 Ma - <660 Ma; Preiss et al., 2011), in this region culminating in development of the Barratta Trough depocentre (Fig. 2). The studied sections to the west and south-west of this trough may thus be considered shallower 'shelf' deposits (Preiss et al., 1993), accumulating within neighbouring sub-basins. The sediments subsequently underwent intracratonic deformation during the Cambrian-Ordovician Delamerian Orogeny, becoming incorporated in a series of continuous, relatively upright fold structures at the

northern margin of the Nackara Arc (Preiss, 2000). The rocks of the study area are characterised by low grade, greenschist facies metamorphism (Preiss, 1995). The minimal metamorphic overprint thus permits detailed study of primary sedimentary facies and structures.

Facies analysis

Data are presented from three detailed logged sections at Holowilena Creek, Oladdie Creek and Hillpara Creek (Fig. 4). Exposure of the underlying Burra Group sediments permits regional correlation, whereas the overlying Tapley Hill Formation is only recorded at Oladdie Creek. Therefore, only minimum thicknesses are observed at Holowilena and Hillpara Creeks, although considerable thickness variations across the logged sections are demonstrable by correlation. Five facies associations are recognized, namely (i) diamictite and conglomerate, (ii) interbedded heterolithics, (iii) hummocky cross-stratified sandstone, (iv) lonestone-bearing siltstone, and (v) ferruginous siltstone and sandstone.

Diamictite and conglomerate facies association

This facies association makes up almost the entire section at Hillpara Creek, is notably dominant at Oladdie Creek, and constitutes less than 50% of the succession at Holowilena Creek. It is sandy throughout, and predominantly crudely stratified, with subsidiary massive and well stratified varieties. The conglomerate deposits commonly display normal grading, fining into diamictite deposits, whilst the latter include normal, reverse and non-graded varieties (Fig. 4). Erosive contacts are prevalent at the base of conglomerates and clast-rich diamictites (Fig. 5a). Outsized clasts range from *c.* 3-80 cm in size, typically 15-20 cm, and comprise limestone, dolostone, metasediments, basalt and granite. Clasts are predominantly sub-angular to sub-rounded in shape; striated forms locally occur.

Downwarping and puncturing of laminae beneath pebble to boulder sized clasts is common (Fig. 5b, c), particularly in the crudely stratified diamictites. Other outsized clasts frequently form turbate structures, where smaller clasts form circular alignments around a core stone or rigid matrix (Fig. 5d, e), and are especially common where downwarping structures are rare. Lenticular siltstone and sandstone bodies locally occur, and are typically bed-parallel. However in places these lenses are highly deformed, forming tight to recumbent intrabed fold structures.

Interpretation. The diamictite and conglomerate facies association is interpreted as a series of glacially-influenced, subaqueous sediment flow deposits. The common fining-upward motif and internal organisation of stacked conglomerate and diamictite deposits is typical of turbulence within the flow (Talling et al. 2012), representing high-density and more dilute turbidites, respectively. This is supported by the abundance of turbate structures, attributed to the generation of transient rotational eddies during turbulent flow (Phillips, 2006). Similar structures can be generated during subglacial shearing of diamictites (e.g. Busfield & Le Heron 2013, and refs within), but this interpretation is deemed unlikely in the absence of other shear-related features e.g. attenuated clasts, pressure shadows, galaxy structures. Massive and reverse graded diamictite deposits are interpreted as the product of glaciogenic debris flows (GDFs), which commonly generate inverse grading patterns through the combined influence of upward clast migration and kinetic sieving (Legros, 2002; Benn & Evans, 2010; Talling et al., 2012). Erosive contacts at the base of many conglomerate and clast-rich diamictite units reflects repeated sediment flow emplacement, and resultant cannibalisation of underlying sediments.

The close association of GDFs and turbidites likely reflects flow transformation during downslope movement, whereby mixing of the subaqueous debris flow with the overlying water body results in flow dilution (Benn & Evans, 2010; Talling et al., 2012), and hence a tendency towards more turbulent flow conditions. The generation of these ‘linked’ turbidity currents frequently occurs through transformation of moderate strength debris flows (Talling et al., 2012), and is a common

process within ice-proximal and ice-contact regimes under rates of high sedimentation (Benn & Evans, 2010). This is consistent with the occurrence of tight to recumbent folded sand lenses, associated with slumping and sediment failure in response to rapid sediment delivery (Maltman, 1994). Outsized clasts which downwarp and puncture underlying laminae are interpreted as ice-rafted debris (IRD), wherein the preserved examples likely accumulated as sediment flows waned, thus restricting overprint of the structures under downslope remobilisation. The local occurrences of striated clasts provide further credence to the proposed glacigenic origin.

Interbedded heterolithics facies association

This facies association comprises a series of well stratified, dominantly interbedded siltstones, fine sandstones and coarse quartz arenites. It is most prominent in the Holowilena Creek section, constituting approximately 30% of the succession, diminishing to <10% in the Oladdie Creek deposits and *c.* 2% at Hillpara Creek (Fig. 4). No lonestones occur within this facies association. The deposits exhibit minimal grading; rarely sandstone interbeds fine upward into the overlying siltstone. Current ripple cross-lamination is common within the fine sandstone-siltstone interbeds (Fig. 6a), predominantly demonstrating palaeoflow towards the north. An isolated example of climbing ripple cross-lamination is recorded at Oladdie Creek. In places, the fine sandstone interbeds are deformed into largely bed-parallel discontinuous fold structures (Fig. 6b), other beds contain highly convolute lamination as well as load and flame structures (Fig. 6c). Conversely, the coarser quartzite interbeds are planar throughout, and exhibit no sedimentary structures at Holowilena or Oladdie, with limited evidence of small-pebble lined cross-bedding in the Hillpara Creek section (at ~75 m Log C, Fig. 4).

Interpretation. The interbedded heterolithics facies association is interpreted as a finer grained series of sediment flow deposits, wherein the enhanced preservation of bedforms likely reflects reduced sediment concentrations compared to the coarser diamictite and conglomerate facies

association. This may be a product of diminished sediment supply, which in tandem with the loss of the ice-rafting signature can be used to support periods of relative ice margin stability or retreat during deposition of the interbedded heterolithics. Within the coarser grained diamictite and conglomerate facies association, higher sediment concentrations and fall-out rates suppress the migration and preservation of delicate ripple structures (Sumner et al., 2008; Talling et al., 2012). However, as they move downslope, flows become more dilute through mixing with the water column, generating fully turbulent, low-density flows that enable the development of ripple cross-lamination (Baas et al., 2011; Talling et al., 2012). Rare normally-graded sandstone interbeds are likewise interpreted to record deposition from turbulent underflows, succeeded by settling of hemipelagic silt material as the flows waned (e.g. Allen et al., 2004). The preservation of convolute lamination and climbing ripple cross-lamination at intervals reflects periods of more rapid turbidite deposition (Kuenen & Humbert, 1969; Allen, 1991; Baas, 2000; Jobe et al., 2012; Talling et al., 2012). Similarly, folded sandstone and siltstone beds/lenses attest to downslope slumping and sediment instability induced by rapid sedimentation (Maltman, 1994). Load and flame structures attest to Rayleigh-Taylor instabilities initiated at a grain-size/bed interface (Allen, 1984; Collinson and Thompson, 1987).

The coarser quartz arenite beds typically lack internal organisation, and are thus interpreted as non- or poorly-cohesive, clean sand debrites (Talling et al., 2012). An alternative mechanism of incremental accumulation via high-density turbidity currents is rejected owing to the absence of vertical and lateral grading (Kneller & Branney, 1995; Talling et al., 2012). Moreover, the prominent cross-bedded quartzite bed at Hillpara Creek (at ~75 m Log C, Fig. 4) pinches out sharply as opposed to gradationally, considered a characteristic feature of debris flow deposition (Johnson, 1970; Major & Iverson, 1999; Amy et al., 2005; Amy & Talling, 2006). The generation of dune-scale traction bedforms is also incompatible with rapid deposition from a high-density turbidity current (Kuenen, 1966; Middleton & Hampton, 1973; Talling et al., 2012). The prominent

quartzite bed at Hillpara has been previously interpreted as a large ice-rafted erratic (Binks, 1968). However, in light of its bed-parallel orientation, the absence of associated impact-related deformation and its textural similarity to other quartzite interbeds at Holowilena and Oladdie, we prefer interpretation as a laterally discontinuous debrite.

Hummocky cross-stratified sandstone facies association

This facies association is restricted to the Holowilena Creek section (Log A, Fig. 4). Overall, the facies resemble those of the interbedded heterolithics facies association in that they comprise well stratified, non-graded fine sandstone and siltstone interbeds. They are distinguished, however, by the occurrence of hummocky cross-stratification (HCS) within many of the sandstone units (Fig. 6d-e). The bedforms are predominantly isotropic, with subsidiary anisotropic components. Current ripple cross-laminated and convolute laminated sandstones are also intercalated within this facies association. Lonestones were not observed.

Interpretation. The interbedded current rippled sandstones and laminated siltstones are interpreted to record turbulent underflow deposition and settling of hemipelagic fines, respectively, in concert with the interbedded heterolithics facies association. However, the presence of HCS attests to the interplay of storm wave oscillatory flow during deposition, within a shallow shelf environment (Cheel & Leckie, 1993; Johnson & Baldwin, 1996; Duke et al., 1991; Dumas & Arnott, 2006). Le Heron et al. (2011a, b) argue in favour of sea ice-free conditions at this time, as sea ice would inhibit the efficacy of storm wave agitation. Certainly these features attest to a sea ice minimum zone, where sufficient expanses of open water enable storm wave agitation, although the extent of ice meltback remains unclear. The absence of lonestones within this facies association is consistent with a lack of glacial influence on deposition.

Lonestone-bearing siltstone facies association

This facies association consists predominantly of planar laminated siltstone, with notably fewer sandstone beds than the interbedded heterolithics facies association. It is restricted to the Holowilena and Oladdie Creek sections, constituting <10% and <5% of the succession, respectively (Fig. 4). Downwarping of laminae beneath the outsized lonestones is common, in places piercing the laminae also (Fig. 6f). Rarely, lamina-parallel trains of lonestones are recorded, coincident with the absence of downwarping features.

Interpretation. The predominance of planar laminated siltstone alongside minor sandstone interbeds is interpreted to record settling of hemipelagic fines, interrupted by isolated sand-rich sediment underflows. The presence of outsized lonestones which puncture and downwarp underlying laminae provides clear evidence of ice-rafting during deposition. Sediment flow 'rafting' of the lonestones (e.g. Postma et al., 1988; Eyles & Januszczak, 2007) is discounted on the basis of the fine grain size of the supporting material, which would lack the cohesive strength to transport cobble to boulder sized material.

Ferruginous siltstone and sandstone facies association

This facies association is again restricted to Holowilena Creek, and attains only 6 m in thickness in the studied section (Log A, Fig. 4). It comprises both massive and crudely stratified fine sandstone and siltstone, with few granule to small pebble sized clasts, which are locally associated with impact-related deformation at the micro-scale (Fig. 6g). No pebble or boulder sized lonestones were observed within this facies association. Sharp, undulose, bed-parallel layering is apparent in the siltstone unit (Fig. 6h), alongside an isolated asymmetric fold structure verging towards the south-east (Fig. 6i).

Interpretation. The ferruginous siltstone and sandstone facies association is tentatively interpreted to record similar styles of hemipelagic silt deposition and underflow sand emplacement as the lonestone bearing siltstone facies association. However, impact-related deformation beneath granule

sized clasts at the micro-scale is interpreted to record early onset of ice-rafting processes. It is possible that the bed-parallel, undulose layering (Fig. 6h) may represent horizontal algal laminites, and by association an algal growth structure preserved in the asymmetric fold. This tentative interpretation is based on recognition of similar features observed in age-equivalent deposits of northern Namibia (Le Heron et al., 2013), but requires further investigation.

The source of iron minerals within Neoproterozoic glacial successions remains highly contentious, and is considered beyond the scope of this study given its limited outcrop occurrence. Recent studies in South Australia support the intermixing of detrital terrestrial sediment and hydrothermal fluids (Lottermoser & Ashley, 2000; Cox et al., in press). In contrast to previous studies which advocate globally-widespread seawater anoxia (e.g. Kirschvink, 1992), the accumulation of abundant soluble iron, and hence deposition of iron-enriched sediments, is thought to occur under enhanced, not extreme anoxia and elevated Fe:S ratios (Cox et al., in press).

Depositional cycles and glacial sequence stratigraphy

The preceding facies analysis reveals a diverse accumulation of sediments both with and without evidence of glacial influence on deposition. Examination of the vertical grading of these facies associations, alongside changes in their lateral distribution, provides insight into their depositional history, and enables a sequence stratigraphic framework to be constructed. Sequence stratigraphic concepts are scarcely applied to glacial depositional systems (e.g. Proust & Deynoux, 1994; Brookfield & Martini, 1999; Powell & Cooper, 2002; El-ghali, 2005; Pedersen, 2012), largely due to the complexity of deciphering the influence of glacial fluctuations from changes in relative lake/sea-level. The term ‘glacial sequence stratigraphy’ is therefore used to denote a sequence stratigraphic model driven by glacier dynamics (Powell & Cooper, 2002), the effects of which are preserved independently of other external forces e.g. eustacy, isostacy. Glacial systems tracts (GST) are defined following the scheme of Powell & Cooper (2002). Systems tracts are subdivided into

glacial advance (GAST) and glacial retreat (GRST) sequences, which may also include ice maximum (GMaST) and ice minimum (GMiST) conditions, respectively. Ten glacial systems tracts are recognized (Fig. 7), separated either by a glacial erosion surface (GES) or glacial bounding surface (GBS), the latter including the glacial advance surface (GAS) representing the onset of advance systems tracts, and the iceberg-rafting termination surface (ITS) representing the onset of retreat.

The first sequence is restricted to the base of the Holowilena Creek section (Fig. 7), and constitutes striated clast-bearing sediment gravity flow deposits of the diamictite and conglomerate facies association, correlated to the Pualco Tillite. This sequence is attributed to the glacial advance systems tract (GAST 1) due to its characteristically thin exposure, and coarsening-upward motif (Powell & Cooper, 2002). The sequence is capped by an onlap surface, representing the first glacial bounding surface (*GBS1*), beneath sediments of the interbedded heterolithics facies association (Fig. 8a). This onlap surface is interpreted to reflect transgression following local ice meltback, demarcating the base of the first glacial retreat systems tract (GRST 1), consistent with the absence of glacigenic indicators (e.g. IRD) in the overlying heterolithic facies (Fig. 7). These sediments are overlain by the ferruginous siltstone and sandstone facies association, the Holowilena Ironstone. The first appearance of micro-scale IRD at this interval is interpreted as the glacial advance surface (*GAS1*; Powell & Cooper, 2002), and thus the overlying Holowilena Ironstone is interpreted as a thinly exposed remnant of the second GAST.

The top of the Holowilena Ironstone is sharply truncated by a glacial erosion surface (*GES1*) in the Holowilena Creek section (Figs. 7 & 8b); a widely recognized disconformity throughout the Flinders Ranges (e.g. Coats, 1981; Preiss et al. 1993). The thin exposure of the underlying GAST 2 likely reflects significant downcutting during development of the GES. The surface is correlated to the top of the pre-glacial Burra Group sediments at Oladdie Creek and Hillpara Creek based upon the absence of the underlying Pualco Tillite and Holowilena Ironstone, although no significant

erosion surface was observed. The absence of a significant erosion surface in the proximal sections is likely attributed to re-working and erosion during subsequent sediment flow emplacement (during GRST 2), as opposed to marine ravinement, the effects of which would be expected to be more prominent in the distal sections, and accompanied by a transgressive lag, which is not present. Deposits of the glacial maximum systems tract (GMaST) are not recorded above the GES, as is typical of many temperate glacial systems (Powell & Cooper, 2002). Instead, at Holowilena and Oladdie, the overlying sediments of the Wilyerpa Formation correspond to a second phase of glacial retreat (GRST 2, Fig. 7). These comprise stacked, dominantly fining-upward deposits of the diamictite and conglomerate facies association and interbedded heterolithics facies association. The former contains repeated intervals of IRD, which are typically absent in the latter. This is interpreted as the product of pulsed collapse events at the ice front, driving coarser grained gravity flows and iceberg distribution into the basin, followed by periods of relative ice margin stability or retreat. During these intervals, the shelf becomes starved of coarser sediment, leading to deposition of finer grained sediment flow deposits, and ice-rafting processes are inhibited.

Transition to an advance systems tract (GAST 3) is recorded above this sequence (at *GBS2*, Fig. 7), where coarser grained sediments of the diamictite and conglomerate facies association pre-dominate, concomitant with a switch to a coarsening-upward motif. A pronounced inverse-grading event can be correlated across all three logged sections (Fig. 7: 260 m Log A, 62 m Log B, 18 m Log C), and at Holowilena is accompanied by a sudden influx of exotic pebble to boulder sized granite clasts (Fig. 8c). This event is interpreted to record ice maximum conditions (GMaST), resulting in high rates of sediment supply and delivery of extrabasinal erratic lithologies. At Holowilena and Oladdie a thin succession of normally-graded diamictite and conglomerate facies above *GBS3* mark a return of the GRST (3), capped by an abrupt facies dislocation to thinly laminated siltstones (Fig. 7). This facies change is concurrent with the disappearance of IRD, and is thus identified as the iceberg-rafting termination surface (*ITS1*; Powell & Cooper, 2002).

The retreat sequence above *ITS1* is largely restricted to the Holowilena Creek section (Fig. 7), and comprises the hummocky cross-stratified sandstone facies association at the base, and interbedded heterolithics facies association above. The occurrence of hummocky cross-stratification in the basal sediments, requiring sufficient open waters and hence sea ice meltback to permit storm wave agitation (Le Heron et al. 2011a, b), is used to support ice minimum conditions (GMiST). Moreover, HCS is typically encountered within a shallow shelf setting (Cheel & Leckie, 1993; Johnson & Baldwin, 1996; Duke et al., 1991; Dumas & Arnott, 2006), and thus the absence of this facies association in the more proximal, shallower Oladdie Creek and Hillpara Creek sections may reflect a period of subaerial exposure and non-deposition in the proximal reaches during this retreat phase. The overlying interbedded heterolithic facies above *GBS4* record an influx of coarser grained sand underflows within the Oladdie and Holowilena Creek sections, interpreted as the product of increased sediment instability in the source region, perhaps in response to initial, more proximal ice movement which may correspond to early GAST. However, the first appearance of IRD in the overlying laminated siltstones is taken as a more reliable indicator of initial advance (Powell & Cooper, 2002), identified as the second glacial advance surface (*GAS2*; Fig. 7).

The overlying GAST 4 is initially characterised by stacked, thickly-bedded IRD-bearing diamictite and conglomerate at Hillpara Creek, normally-graded and thinly bedded diamictite and conglomerate separated by IRD-bearing siltstone at Oladdie Creek, and by IRD-bearing siltstone only at Holowilena Creek (Fig. 7). These facies associations reflect initial advance of the ice front, where coarse-grained glacially-influenced sediment flows are deposited in the more proximal regions (Hillpara), further downslope these sediment flows occur as pulsed events separated by periods of quiescence where ice-rafting processes dominate (Oladdie), and the distal regions remain starved of coarser-grained sediment, preserving only the ice-rafting signature (Holowilena). Towards the top of the succession, above *GBS5*, thickly-bedded and dominantly inverse graded

diamictites, conglomerates and coarse-grained sandstones are preserved across all three logged sections, reflecting full glacial advance during late stage GAST 4, identified as the GMaST (Fig. 7).

The upper contact of the Wilyerpa Formation, and cessation of glacially-influenced sedimentation, was observed only in the Oladdie Creek section (Fig. 7). Here, an erosional contact occurs at the base of a pebble to boulder-bearing conglomerate, with a distinct dark grey silt matrix, notably dissimilar to the pale brown sandy matrix of the underlying Wilyerpa Formation (Fig. 8d). The conglomerate is interpreted as a post-glacial transgressive lag, and is succeeded by a thick succession of laminated dark grey siltstones of the Tindelpina Shale Member, the basal unit of the Tapley Hill Formation.

Discussion

Sequence stratigraphic analysis of the studied sections in the central and southern Flinders Ranges identifies four distinct glacial advance sequences, separated by three intervals of ice meltback (Fig. 7). The glacial influence on deposition (IRD) is pervasive throughout the Hillpara and Oladdie Creek sections. This is consistent with their more proximal position relative to the ice front (see Fig. 9), corroborated by the predominance of coarser grained facies associations, as well as ripple cross-lamination and soft sediment slump folding indicative of sediment supply from the south. The Holowilena Creek section represents the most ice-distal position, as indicated by the clear increase of fine grained facies. Deposition in the ice-proximal zone is proposed due to the dominance of sediment gravity flow and ice-rafting processes (Benn & Evans, 2010), with sediment accumulation on the shelf at Hillpara and Oladdie, and the slope at Holowilena (Fig. 9).

The studied sections demonstrate considerable thickness variations, thickening by a few tens of metres from Hillpara to Oladdie, and by several hundred metres to Holowilena Creek (Fig. 7). This is attributed to significant palaeotopographic relief during deposition (see Fig. 9), the origin of which remains obscure. Previous studies have advocated accumulation of Sturtian glacigenic

sediments within pre- and early syn-depositional rift basins (e.g. Preiss, 2000), whilst the presence of a distinct glacial erosion surface immediately above the Holowilena Ironstone may be used to support the interplay of subglacial downcutting (sensu Young & Gostin, 1990, 1991). Nonetheless, the palaeotopographic depression at Holowilena provided enhanced accommodation space for the preservation of non-glacially influenced regressive systems tracts, alongside protection from cannibalization under repeated sediment flow emplacement. In contrast, on the palaeotopographic highs at Oladdie and Hillpara (Fig. 9), relatively thin successions of stacked coarse-grained sediment flows likely underwent significant cannibalization and re-working during subsequent downslope movements, re-deposited basinward as flows waned, and hence glacial advance systems tracts are preferentially preserved.

Previous studies in South Australia have also identified multiple advance-retreat sequences within the Sturtian record (e.g. Forbes, 1970; Forbes & Cooper, 1976; Coats & Preiss, 1987; Young & Gostin 1988, 1989, 1990, 1991; Le Heron et al., 2011b). The four-fold stratigraphic subdivision of Young & Gostin (1990, 1991) comprises two diamictite-dominated intervals, each overlain by mudstone-dominated facies, interpreted as glacial advance and retreat sequences, respectively. The uppermost mudstone-dominated interval, Unit 4 of Young & Gostin (1990), is regarded as a transitional unit between the diamictic deposits of Unit 3 and the shale-rich deposits of the post-glacial Tapley Hill Formation. These considerations suggest the diamictites of the upper GMaST in the central and southern Flinders Ranges, overlain by the Tapley Hill Formation at Oladdie Creek (Fig. 7), correlate with Unit 3 of Young & Gostin (1990, 1991), and therefore Unit 4 is absent. The absence of Unit 4 from sequences in the Northern Flinders Basin (Young & Gostin, 1990) is attributed to non-deposition on topographically elevated regions, possibly in response to local tectonic and/or isostatic readjustments. This is considered plausible following the significant glacial advance recorded in the upper GMaST (this study) and Unit 3 (Young & Gostin, 1990, 1991). Furthermore, the basal GAST 1 and GRST 1 identified in the Holowilena Creek section are not

391 recorded by Young & Gostin (1990, 1991). Previous studies in the Olary region to the east of the
392 Orroroo map sheet, however, also recognize the basal Pualco Tillite as recording the glacial
393 maximum of the first Sturtian glaciation (Forbes, 1989; Coats & Preiss, 1987). The absence of these
394 depositional sequences in the Northern Flinders Basin may reflect erosion during subglacial
395 downcutting, coeval with GES 1 at the top of the Holowilena Ironstone (Figs. 7-9).

396 In the North Flinders Basin, Le Heron et al. (in press) recently interpreted a trough mouth fan
397 (TMF) in the Sturtian glacigenic record, building out seaward of a small palaeo-ice stream. Three
398 facies associations are recognized, comprising a diamictite facies association accumulating via
399 glaciogenic debris flows and ice-rafting processes at the ice margin, a channel belt facies
400 association recording channelized turbidity currents subject to ice-rafting on the proximal and
401 medial areas of the fan, and a sheet heterolithics facies association, deposited as non-channelized
402 turbidites and ice-rafted debris. The overriding signature of sediment gravity flow deposition
403 subject to ice-rafting processes closely mirrors the depositional sequences described in this study.
404 The sequences are readily differentiated, however, on the abundance of coarse-grained material.
405 The Bolla Bollana Formation (Le Heron et al. in press) is dominated by coarse grained diamictite
406 and conglomerate facies, with a subordinate fines component throughout, and hence records
407 deposition principally as sediment concentrated glaciogenic debris flows (GDFs). Our present
408 study, meanwhile, demonstrates significantly greater facies variability, a more diverse range of
409 grain sizes throughout, and a notably more abundant component of fines. As a result, the dominant
410 mode of deposition is via less concentrated turbulent sediment flows. Le Heron et al. (in press)
411 correlated the Bolla Bollana Formation to the second glacial advance (Unit 3) of Young & Gostin
412 (1991), which would therefore equate to the upper GMaST of this study. This is consistent with
413 build-out of TMFs during glacial advance (e.g. Powell & Cooper, 2002; Ó'Cofaigh et al., 2012).
414 The North Flinders Basin is, however, widely considered as a separate sub-basin, disconnected from
415 the depocentres of the central and southern Flinders Ranges (Preiss 1987, 2000; Preiss et al. 2011).

Arguably, therefore, separate ice masses may have fed each depocentre, where the evidence for concomitant advance phases, each following a period of significant ice meltback, may testify to regional warming and cooling events.

To summarise, this study proposes multiple, clear-cut cycles within the Sturtian glaciation of South Australia. Whilst the concept of hydrological shutdown under the snowball Earth hypothesis (Hoffman et al., 1998; Hoffman & Schrag, 2002) is readily dismissed from sedimentological evidence (Allen and Etienne, 2008), the true nature of ice sheet dynamics have awaited clairification. Despite having received very few attempts to apply it in the Cryogenian, sequence stratigraphic analysis is clearly a valuable tool to elucidate glacial cycles, including recognition of open water during glacial minima. Detailed examination of the sections at Holowilena Creek, Oladdie Creek and Hillpara Creek therefore contribute to the growing body of research supporting a dynamic Neoproterozoic cryosphere, akin to the numerous Phanerozoic icehouse events recorded throughout Earth's history (e.g. Etienne et al., 2007; Allen & Etienne, 2008; Arnaud et al., 2011 and refs therein). Contingent on an adequate chronostratigraphic framework, detailed facies and sequence stratigraphic analysis of pan-global 'Sturtian' successions may even allow the glaciodynamic signature of these successions to be assessed on a global scale.

Conclusions

Detailed sedimentary logging of previously little described sections in Holowilena Creek, Oladdie Creek and Hillpara Creek in the central and southern Flinders Ranges reveals significant lateral and vertical facies variation within the Yudnamutana Subgroup. Repeated occurrences of ice-rafted debris and subglacially striated clasts attest to a strong glacial influence on sedimentation. The application of glacial sequence stratigraphy enables the dynamics of the Sturtian ice sheet to be elucidated:

- Five facies associations are recognized: 1) Diamictite and conglomerate facies association (glaciogenic debris flows and turbidites subject to secondary ice-rafting), 2) Interbedded heterolithics facies association (debrites, low-density turbidites and hemipelagic fines), 3) Hummocky cross-stratified sandstone facies association (storm-wave agitation of low-density turbidity currents and settling of hemipelagic fines), 4) Lonestone-bearing siltstone facies association (settling of hemipelagic fines and isolated sand-rich turbulent underflows), and 5) Ferruginous siltstone and sandstone facies association (settling of hemipelagic fines and sand-rich turbulent underflows under enhanced anoxia, subject to subordinate ice-rafting).

- Thickness variations across the logged sections attest to an irregular underlying palaeotopography during deposition, attributed to the combined influence of pre- and early syn-depositional rift activity and subglacial downcutting.

- Glacial sequence stratigraphic analysis identifies four glacial advance systems tracts (GAST), separated by three glacial retreat systems tracts (GRST), the uppermost GRST 3 testifying to open water conditions. These findings support dynamic advance and retreat of the Sturtian ice sheet, requiring an active hydrological cycle.

Acknowledgements

The authors are extremely grateful to Alan S Collins (University of Adelaide) and Benjamin L Moorhouse (University of Otago) for their assistance in the field. We would like to thank the two anonymous reviewers for suggestions which allowed us to improve the manuscript, Anthony Spencer for constructive comments on an earlier draft of the manuscript, and the editorial input of Philip Hughes. This work was funded by the National Geographic Explorer Fund, Novas Consulting Research Grant (Geological Society, London), Gill Harwood Memorial Fund (BSRG) and the Helen Shackleton Award (RHUL).

References

ALLEN, J.R.L. 1984. *Sedimentary Structures: Their Character and Physical Basis, volumes I and II*. Elsevier, Amsterdam, 593 p.

ALLEN, J.R.L. 1991. The Bouma A division and the possible duration of turbidity currents. *Journal of Sedimentary Petrology*, **61**, 291-295.

ALLEN, P.A. & ETIENNE, J.L. 2008. Sedimentary challenge to Snowball Earth. *Nature Geoscience*, **1**, 817-825.

ALLEN, P.A., LEATHER, J. & BRASIER, M.D. 2004. The Neoproterozoic Fiq glaciation and its aftermath, Huqf supergroup of Oman. *Basin Research*, **16**, 507-534.

AMY, L.A. & TALLING, P.J. 2006. Anatomy of turbidite and debrite sandstones based on long distance (120 x 35 km) bed correlation, Marnoso-arenacea Formation, Northern Appenines, Italy. *Sedimentology*, **53**, 161-212.

AMY, L.A., TALLING, P.J., PEAKALL, J., WYNN, R.B. & ARZOLA THYNNE, R.G. 2005. Bed geometry used to test recognition criteria of turbidites and (sandy) debrites. *Sedimentary Geology*, **79**, 163-174.

ARNAUD, E., HALVERSON, G.P. & SHIELDS-ZHOU, G. (eds.) 2011. *The Geological Record of Neoproterozoic Glaciations*. Geological Society, London, Memoirs, **36**, 752 p.

BAAS, J.H. 2000. Duration of deposition from decelerating high-density turbidity currents. *Sedimentary Geology*, **136**, 71-88.

BAAS, J.H., BEST, J.L. & PEAKALL, J. 2011. Depositional processes, bedform development and hybrid flows in rapidly decelerated cohesive (mud-sand) sediment flows. *Sedimentology*, **58**, 1953-1987.

BENN, D.I. & EVANS, D.J.A. 2010. *Glaciers and Glaciation*. Hodder Education, London, 802 p.

BINKS, P.J. 1968. *Orroroo Sheet SI54-1*. 1:250,000 scale Geological Map and Explanatory Notes, Primary Industries and Resources South Australia.

BROOKFIELD, M.E. & MARTINI, I.P. 1999. Facies architecture and sequence stratigraphy in glacially influenced basins: basic problems and water-level/glacier input-point controls (with an example from the Quaternary of Ontario, Canada). *Sedimentary Geology*, **123**, 183-197.

BUSFIELD, M.E. & LE HERON, D.P. 2013. Glacitectonic deformation in the Chuos Formation of northern Namibia: implications for Neoproterozoic ice dynamics. *Proceedings of the Geologists Association*, **124**, 778-789.

CHEEL, R.J. & LECKIE, D.A. 1993. Hummocky cross-stratification. *In:* Wright, V.P. (ed.) *Sedimentology Review*. Wiley Blackwell, London, 103-122.

COATS, R.P. 1981. Late Proterozoic (Adelaidean) tillites of the Adelaide Geosyncline. *In:* HAMBREY, AND M.J., HARLAND, W.B. (eds.) *Earth's Pre-Pleistocene Glacial Record*. Cambridge University Press, Cambridge, 537-548.

COATS, R.P. & PREISS, W.V. 1987. Stratigraphy of the Umberatana Group. *In:* PREISS, W.V., (ed.) *The Adelaide Geosyncline: Late Proterozoic Stratigraphy, Sedimentation, Palaeontology and Tectonics*. Geological Survey of South Australia, Bulletin 53, 125-210.

COLLINSON, J.D. & THOMPSON, D.B. 1987. *Sedimentary Structures*, 2nd edition. Chapman and Hall, London.

CONDON, D.J. & BOWRING, S.A. 2011. A user's guide to Neoproterozoic geochronology. *In:* ARNAUD, E., HALVERSON, G.P., SHIELDS-ZHOU, G. (eds.) *The Geological Record of Neoproterozoic Glaciations*. Geological Society, London, Memoirs, **36**, 135-149.

COX, G.M., HALVERSON, G.P., MINARIK, W.G., LE HERON, D.P., MACDONALD, F.A., BELLEFROID, E.J. & STRAUSS, J.V. *in press*. Neoproterozoic Iron Formation: an evaluation of its temporal, environmental and tectonic significance. Chemical Geology, http://dx.doi.org/10.1016/j.chemgeo.2013.08.002

DUKE, W.L., ARNOTT, R.W.C. & CHEEL, R.J. 1991. Shelf sandstones and hummocky cross-stratification: new insights into a stormy debate. *Geology*, **19**, 625-628.

DUMAS, S. & ARNOTT, R.W.C. 2006. Origin of hummocky and swaley cross-stratification – the controlling influence of unidirectional current strength and aggradation rate. *Geology*, **34**, 1073-1076.

EL-GHALI, M.A.K. 2005. Depositional environments and sequence stratigraphy of the paralic glacial, para-glacial and postglacial Upper Ordovician siliciclastic deposits of the Murzuq Basin, SW Libya. *Sedimentary Geology*, **177**, 145-173.

ETIENNE, J.L., ALLEN, P.A., RIEU, R. & LE GUERROUÉ, E. 2007. Neoproterozoic glaciated basins: a critical review of the Snowball Earth hypothesis by comparison with Phanerozoic glaciations. *In:* HAMBREY, M.J., CHRISTOFFERSEN, P., GLASSER, N.F. & HUBBARD, B. (eds.) *Glacial Sedimentary Processes and Products*. Blackwell Publishing Ltd., Oxford, 343-399.

EYLES, N. & JANUSZCZAK, N. 2007. Syntectonic subaqueous mass flows of the Neoproterozoic Otavi Group, Namibia: where is the evidence of global glaciation? *Basin Research*, **19**, 179-198.

FANNING, C.M. & LINK, P.K. 2006. Constraints on the timing of the Sturtian glaciogene event from southern Australia; i.e. for the true Sturtian. *Geological Society of America Abstracts with Programs*, **38**, no. 7, p. 115.

FORBES, B.G. 1970. Benda Siltstones. *Geological Survey of South Australia, Quarterly Notes*, **33**, 1-2.

FORBES, B.G. 1989. *Olary Sheet SI54-2*. 1:250,000 scale Geological Map and Explanatory Notes, Primary Industries and Resources South Australia.

FORBES, B.G. & COOPER, R.S. 1976. The Pualco Tillite of the Olary region, South Australia. *Geological Survey of South Australia, Quarterly Notes*, **60**, 2-5.

GRADSTEIN, F.M., OGG, J.G. & SMITH, A.G. (eds) 2004. *A Geologic Time Scale*. Cambridge University Press, 589 p.

HOFFMAN, P.F. & SCHRAG, D.P. 2002. The snowball Earth hypothesis: testing the limits of global change. *Terra Nova*, **14**, 129-155.

HOFFMAN, P.F., KAUFMAN, A.J., HALVERSON, G.P. & SCHRAG, D.P. 1998. A Neoproterozoic snowball Earth. *Science*, **281**, 1342-1346.

HOWCHIN, W. 1901. Preliminary note on the existence of glacial beds of Cambrian age in South Australia. *Transactions of the Royal Society of South Australia*, **25**, 10-13.

HOWCHIN, W. 1908. Glacial beds of Cambrian age in South Australia. *Quarterly Journal of the Geological Society*, **64**, 234-259.

JOBE, Z.R., LOWE, D.R. & MORRIS, W.R. 2012. Climbing-ripple successions in turbidite systems: depositional environments, sedimentation rates and accumulation times. *Sedimentology*, **59**, 867-898.

JOHNSON, A.M. 1970. *Physical Processes in Geology*. Freeman Cooper, San Francisco, 577 p.

JOHNSON, H.D. & BALDWIN, C.T. 1996. Shallow clastic seas. In: READING, H.G. (ed) *Sedimentary Environments*. Blackwell, London, pp. 236-286.

KENDALL, B., CREASER, R.A. & SELBY, D. 2006. Re-Os geochronology of postglacial black shales in Australia: constraints on the timing of 'Sturtian' glaciation. *Geology*, **34**, 729-732.

KIRSCHVINK, J.L. 1992. Late Proterozoic low-latitude glaciation: the snowball Earth. *In:* SCHOPF, J.W., AND KLEIN, C. (eds.) *The Proterozoic Biosphere*. Cambridge University Press, Cambridge, 51-52.

KNELLER, B.C. & BRANNEY, M.J. 1995. Sustained high-density turbidity currents and the deposition of thick massive sands. *Sedimentology*, **42**, 607-616.

KUENEN, P.H. 1966. Experimental turbidite lamination in a circular flume. *The Journal of Geology*, **74**, 523-545.

KUENEN, P.H. & HUMBERT, F.L. 1969. Grain size of turbidite ripples. *Sedimentology*, **13**, 253-261.

LE HERON, D.P. 2012. The Cryogenian record of glaciation and deglaciation in South Australia. *Sedimentary Geology*, **243-244**, 57-69.

LE HERON, D.P., COX, G.M., TRUNDLEY, A.E. & COLLINS, A. 2011a. Sea ice-free conditions during the Sturtian glaciation (early Cryogenian), South Australia. *Geology*, **39**, 31-34.

LE HERON, D.P., COX, G.M., TRUNDLEY, A.E. & COLLINS, A. 2011b. Two Cryogenian glacial successions compared: aspects of the Sturt and Elatina sediment records of South Australia. *Precambrian Research*, **186**, 147-168.

LE HERON, D.P., BUSFIELD, M.E., LE BER, E. & KAMONA, A.F. 2013. Neoproterozoic ironstones in northern Namibia: biogenic precipitation and Cryogenian glaciation. *Palaeogeography, Palaeoclimatology, Palaeoecology*, **369**, 48-57.

LE HERON, D.P., BUSFIELD, M.E., COLLINS, A.S. *in press*. Bolla Bollana boulder beds: A Neoproterozoic trough mouth fan in South Australia? Sedimentology (2013) doi: 10.1111/sed.12082.

LEGROS, F. 2002. Can dispersive pressure cause inverse grading in grain flows? *Journal of Sedimentary Research*, **72**, 166-170.

LINK, P.K. & GOSTIN, V.A. 1981. Facies and paleogeography of Sturtian glacial strata (late Precambrian), South Australia. *American Journal of Science*, **281**, 353-374.

LOTTERMOSER, B.G. & ASHLEY, P.M. 2000. Geochemistry, petrology and origin of Neoproterozoic ironstones in the eastern part of the Adelaide Geosyncline, South Australia. *Precambrian Research*, **101**, 49-67.

MAJOR, J.J. & IVERSON, R.M. 1999. Debris-flow deposition: effects of pore-fluid pressure and friction concentrated at flow margins. *Geological Society of America Bulletin*, **111**, 1424-1434.

MALTMAN, A. 1994. *The Geological Deformation of Sediments*. Chapman and Hall, Cambridge, 384 p.

MAWSON, D. 1941. Middle Proterozoic sediments in the neighbourhood of Copley. *Transactions of the Royal Society of South Australia*, **65**, 304-311.

MAWSON, D. 1949. Sturt tillite of Mount Jacob and Mount Warren Hastings, north Flinders Ranges. *Transactions of the Royal Society of South Australia*, **72**, 244-251.

MAWSON, D. & SPRIGG, R.C. 1950. Subdivision of the Adelaide System. *Australian Journal of Science*, **13**, 69-72.

MIDDLETON, G.V. & HAMPTON, M.A. 1973. Sediment gravity flows: mechanisms of flow and deposition. Turbidites and Deep-water Sedimentation, SEPM Pacific Section, Short course lecture notes, p. 1-38.

Ó'COFAIGH, C., ANDREWS, J.T., JENNINGS, A.E., DOWDESWELL, J.A., HOGAN, K.A., KILFEATHER, A.A. & SHELDON, C. 2012. Glacimarine lithofacies, provenance and depositional processes on a West Greenland trough-mouth fan. *Journal of Quaternary Science*, **28**, 13-26.

PEDERSEN, S.A.S. 2012. Glaciodynamic sequence stratigraphy. In: HUUSE, M., REDFERN, J., LE HERON, D.P., DIXON, R.J., MOSCARIELLO, A. & CRAIG, J. (eds.) *Glaciogenic Reservoirs and Hydrocarbon Systems*. Geological Society, London, Special Publications, **368**, 29-51.

PHILLIPS, E. 2006. Micromorphology of a debris flow deposit: evidence of basal shearing, hydrofacturing, liquefaction and rotational deformation during emplacement. *Quaternary Science Reviews*, **25**, 720-738.

POSTMA, G., NEMEC, W. & KLEINSPEHN, K.L. 1988. Large floating clasts in turbidites – a mechanism for their emplacement. *Sedimentary Geology*, **58**, 47-61.

POWELL, R.D. & COOPER, J.M. 2002. A glacial sequence stratigraphic model for temperate, glaciated continental shelves. In: DOWDESWELL, J.A. & O'COFAIGH, C. (eds.) *Glacier-Influenced Sedimentation on High-Latitude Continental Margins*. Geological Society, London, Special Publications, **203**, 215-244.

PREISS, W.V. 1987. A synthesis of palaeogeographic evolution of the Adelaide Geosyncline. In: PREISS, W.V. (ed.) *The Adelaide Geosyncline. Late Proterozoic Stratigraphy,*

Sedimentation, Palaeontology and Tectonics. Geological Survey of South Australia Bulletin, **53**, 315-409.

PREISS, W.V. 1993. Neoproterozoic. In: DREXEL, J.F., PREISS, W.V. & PARKER, A.J. (eds.) *The Geology of South Australia. Volume 1, The Precambrian*. Bulletin 54, Mines and Energy of South Australia. State Print, South Australia, pp. 170-224.

PREISS, W.V. 1995. Delamerian Orogeny. *In:* DREXEL, J.F., AND PREISS, W.V. (eds.) *The geology of South Australia. Vol. 2, The Precambrian*. Geological Survey of South Australia, Bulletin 54, 45-57.

PREISS, W.V. 1999. *Parachilna Sheet SH54-13*. 1:250,000 scale Geological Map and Explanatory Notes, Primary Industries and Resources South Australia.

PREISS, W.V. 2000. The Adelaide Geosyncline of South Australia and its significance in Neoproterozoic continental reconstruction. *Precambrian Research*, **100**, 21-63.

PREISS, W.V., BELPERIO, A.P., COWLEY, W.M. & RANKIN, L.R., 1993. Neoproterozoic. *In:* DREXEL, J.F., PREISS, W.V. & PARKER, A.J. (eds.) *The geology of South Australia. Vol. 1, The Precambrian*. Geological Survey of South Australia, Bulletin 54, 171-203.

PREISS, W.V., DYSON, I.A., REID, P.W. & COWLEY, W.M. 1998. Revision of lithostratigraphic classification of the Umberatana Group. *MESA Journal*, **9**, 36-42.

PREISS, W.V., GOSTIN, V.A., MCKIRDY, D.M., ASHLEY, P.M., WILLIAMS, G.E. & SCHMIDT, P.W. 2011. The glacial succession of Sturtian age in South Australia: the Yudnamutana Subgroup. In: ARNAUD, E., HALVERSON, G.P. & SHIELDS-ZHOU, G. (eds.) 2011. *The Geological Record of Neoproterozoic Glaciations*. Geological Society, London, Memoirs, **36**, 752 p.

PROUST, J.N. & DEYNOUX, M. 1994. Marine to non-marine sequence architecture of an intracratonic glacially-related basin. Late Proterozoic of the West African platform in western Mali. In: DEYNOUX, M., MILLER, J.M.G., DOMACK, E.W., EYLES, N., FAIRCHILD, I.J. & YOUNG, G.M. (eds) *The Earth's Glacial Record: Facies Models and Geodynamic Evolution*. Cambridge University Press, Cambridge, 121-145.

SUMNER, E.J., AMY, L. & TALLING, P.J. 2008. Deposit structure and processes of sand deposition from a decelerating sediment suspension. *Journal of Sedimentary Research*, **78**, 529-547.

TALLING, P.J., MASSON, D.G., SUMNER, E.J. & MALGESINI, G. 2012. Subaqueous sediment density flows: depositional processes and deposit types. *Sedimentology*, **59**, 1937-2003.

YOUNG, G.M. & GOSTIN, V.A. 1988. Stratigraphy and sedimentology of Sturtian glaciogenic deposits in the western part of the North Flinders Basin, South Australia. Precambrian Research, v. 39, p. 151-170.

YOUNG, G.M., AND GOSTIN, V.A. 1989. An exceptionally thick upper Proterozoic (Sturtian) glacial succession in the Mount Painter area, South Australia. *Geological Society of America Bulletin*, **101**, 834-845.

YOUNG, G.M. & GOSTIN, V.A. 1990. Sturtian glacial deposition in the vicinity of the Yankaninna Anticline, North Flinders Basin, South Australia. *Australian Journal of Earth Sciences*, **37**, 447-458.

YOUNG, G.M. & GOSTIN, V.A. 1991. Late Proterozoic (Sturtian) succession of the North Flinders Basin, South Australia; an example of temperate glaciation in an active rift setting. *In:* Anderson, J.R., Ashley, G.M. (eds.) *Glacial Marine Sedimentation: Palaeoclimatic Significance*. Geological Society of America Special Paper, **261**, 207-222.

Figure captions

Figure 1: Geological sketch map of the Adelaide Fold Belt, modified after Preiss (1993), showing location of studied sections. Detailed geological maps of study areas inset; A) Holowilena Creek, modified after Preiss (1999), B) Oladdie Creek and C) Hillpara Creek modified after Binks (1968).

Figure 2: Sketch map demonstrates distribution of Sturtian sedimentary deposits and depositional basins throughout the Adelaide Fold Belt, modified after Preiss et al. (1998). Note location of Barratta Trough and Yudnamutana Trough, representing the principal depocentres during Sturtian glaciation.

Figure 3: Cryogenian stratigraphy and geochronology of the Adelaide Fold Belt and Stuart Shelf, after Preiss et al. (1998). Note disparity in stratigraphic nomenclature of 'Sturtian' glacigenic deposits across South Australia. In this paper data are presented from the Yudnamutana Subgroup of the central and south-west Flinders Ranges.

Figure 4: Logged sections of the Yudnamutana Subgroup in the central and southern Flinders Ranges; A) Holowilena Creek (base of log: 31°59.232'S 138°51.052'E), B) Oladdie Creek (base of log: 32°28.039'S 138°38.285'E), C) Hillpara Creek (base of log: 32°33.777'S 138°47.302'E). Note the variable thickness and lateral distribution of the five facies associations across the logged sections. Significant thickness changes from north to south attest to irregular palaeotopographic relief during deposition.

Figure 5: Representative photographs of the diamictite and conglomerate facies association. (a) Erosive scour at base of normally-graded conglomerate-sandstone interbeds (white triangles demonstrate grading patterns); (b) Ice-rafted dropstone, puncturing and downwarping the underlying laminae. Compaction related deflection above lonestone significantly lower in amplitude than below; (c) Ice-rafted debris with impact related deformation; (d-e) Profile view of rotational turbate structures (circular alignment of clasts around a core stone or rigid matrix). Coin and lens cap for scale measure 2 cm and 5 cm, respectively.

Figure 6: **Interbedded heterolithics facies association:** (a) Fine-grained current ripple cross-laminated sandstone and coarse to granule erosive based sandstone interbeds; (b) Soft-sediment slump folded sandstone interbeds; (c) Trough cross-lamination, convolute laminae and load and flame structures in beds which onlap the underlying Pualco Tillite (see Fig. 8a). **Hummocky cross-stratified sandstone facies association:** (d) Dominantly isotropic hummocky cross-stratified sandstone interbeds, interpretive overlay in (e); (f) Amalgamated sets of isotropic cross strata, with truncation of laminae to the left and above coin. **Lonestone-bearing siltstone facies association:** (g) ice-rafted debris downwarps and punctures underlying silt. **Ferruginous siltstone and sandstone facies association:** (h) Distinct, sharp banding within the Holowilena Ironstone interpreted as possible algal laminites. Note irregular fold structure/possible domed algal laminite, verging towards the south-east. (i) Micro-scale ice-rafted debris which punctures and downwarps underlying laminae. Coin for scale measures 2 cm.

Figure 7: Sequence stratigraphic framework for the studied sections. Glacial systems tracts are separated either by a glacial erosion surface (GES) or glacial bounding surface (GBS), the latter including the glacial advance surface (GAS) and iceberg-rafting termination surface (ITS). Key for glacial systems tracts codes: **GAST**= glacial advance systems tract; **GRST**= glacial retreat systems tract; **GMaST**= glacial maximum systems tract; **GMiST**= glacial minimum systems tract.

Figure 8: Photographs of significant depositional boundaries within the studied succession. (a) Glacially-influenced Pualco Tillite onlapped by non-glacially influenced interbedded heterolithics

(see Fig. 6c); (b) Glacial erosion surface at the base of the Wilyerpa Formation, downcutting into the Holowilena Ironstone; (c) Influx of extrabasinal granite clasts, indicated by white arrows, at inferred glacial maximum; (d) Conglomeratic transgressive lag records terminal glacial conditions at the top of the Wilyerpa Formation, succeeded by post-glacial siltstone of the Tapley Hill Formation. Hammer and lens cap for scale measure 26 cm and 5 cm, respectively.

Figure 9: Simple depositional model for the studied sections in the central and southern Flinders Ranges. Sequence stratigraphic analysis identifies four glacial advance sequences, separated by three intervals of ice meltback. During glacial advance, dynamic ice sheet oscillations drive delivery of glaciogenic debris flows and glacioturbidites downslope, subject to secondary ice-rafting. During glacial retreat, the ice-rafting signature is lost, and ice minimum conditions permit storm-wave agitation of the water column, and generation of hummocky cross-stratified sandstones. Thickness variations across the logged sections attest to significant palaeotopographic relief during deposition, creating progressively greater accommodation space downslope (Hillpara-Oladdie-Holowilena) through the combined effects of pre- and early syn-depositional rift activity and subglacial downcutting. Key for glacial systems tracts codes: **GAST**= glacial advance systems tract; **GRST**= glacial retreat systems tract; **GMaST**= glacial maximum systems tract; **GMiST**= glacial minimum systems tract.

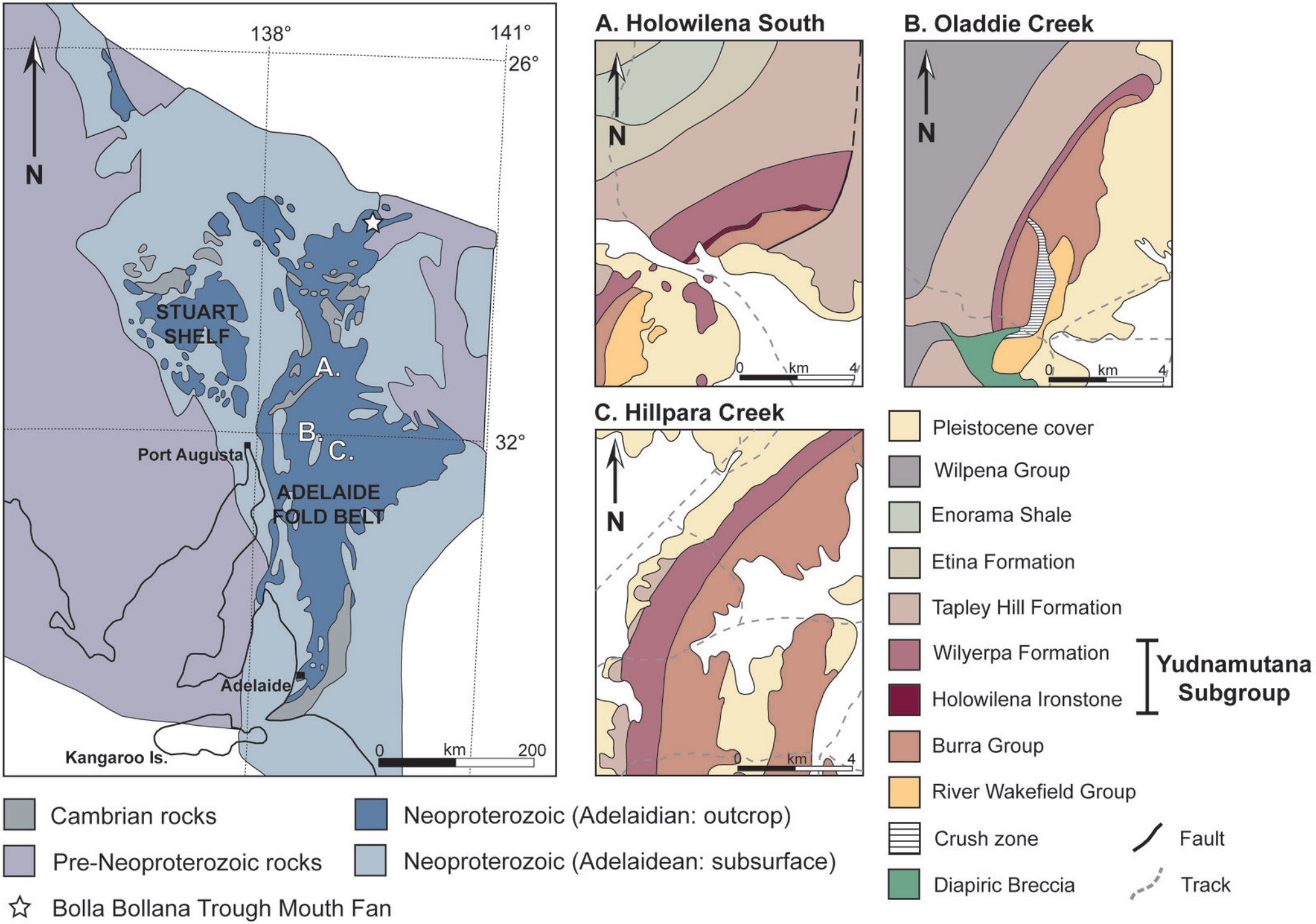
138°
141°
26°
32°
N
STUART SHELF
A.
B.
C.
Port Augusta
ADELAIDE FOLD BELT
Adelaide
Kangaroo Is.
0 km 200
A. Holowilena South
B. Oladdie Creek
C. Hillpara Creek
0 km 4
Pleistocene cover
Wilpena Group
Enorama Shale
Etina Formation
Tapley Hill Formation
Wilyerpa Formation
Holowilena Ironstone
Yudnamutana Subgroup
Burra Group
River Wakefield Group
Crush zone
Diapiric Breccia
Fault
Track
Cambrian rocks
Pre-Neoproterozoic rocks
Bolla Bollana Trough Mouth Fan
Neoproterozoic (Adelaidian: outcrop)
Neoproterozoic (Adelaidean: subsurface)

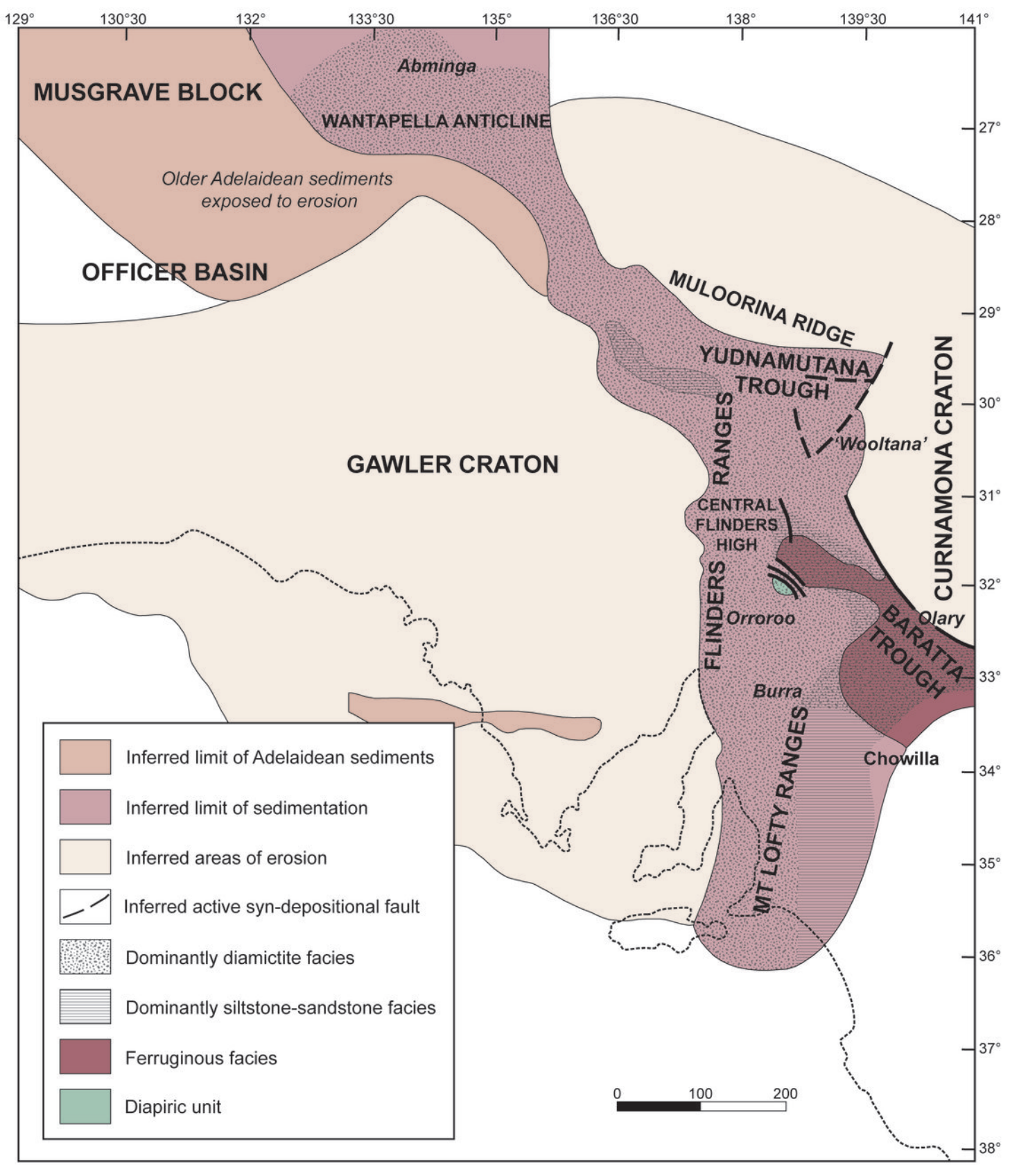
129°
130°30
132°
133°30
135°
136°30
138°
139°30
141°
27°
28°
29°
30°
31°
32°
33°
34°
35°
36°
37°
38°
MUSGRAVE BLOCK
Abminga
WANTAPELLA ANTICLINE
Older Adelaidean sediments exposed to erosion
OFFICER BASIN
MULOORINA RIDGE
YUDNAMUTANA TROUGH
'Wooltana'
CURNAMONA CRATON
GAWLER CRATON
RANGES
CENTRAL FLINDERS HIGH
FLINDERS
Orroroo
Olary
BARATTA TROUGH
Burra
MT LOFTY RANGES
Chowilla
Inferred limit of Adelaidean sediments
Inferred limit of sedimentation
Inferred areas of erosion
Inferred active syn-depositional fault
Dominantly diamictite facies
Dominantly siltstone-sandstone facies
Ferruginous facies
Diapiric unit
0
100
200

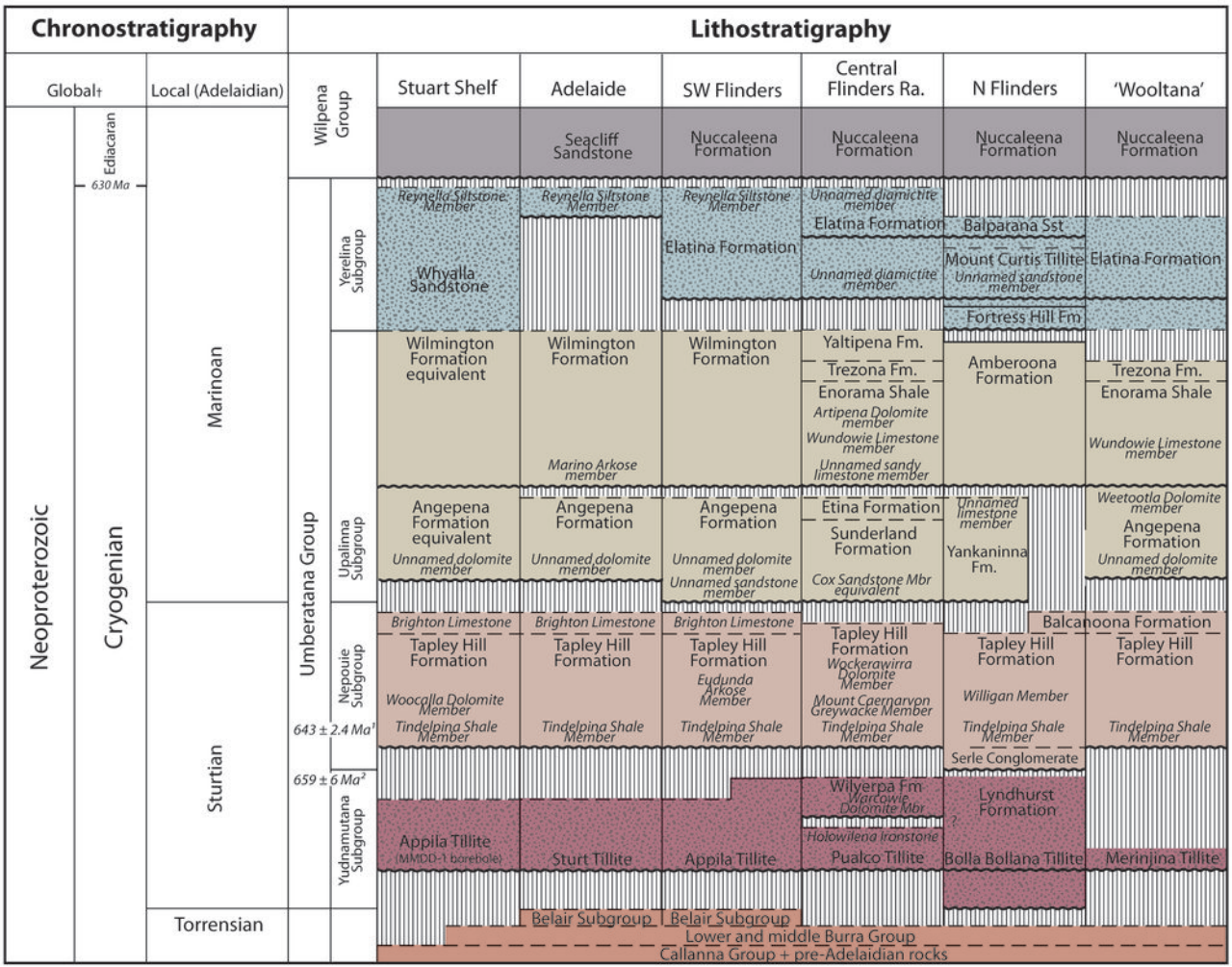
Chronostratigraphy
Lithostratigraphy
Global†
Local (Adelaidian)
Wilpena Group
Stuart Shelf
Adelaide
SW Flinders
Central Flinders Ra.
N Flinders
'Wooltana'
Seacliff Sandstone
Nuccaleena Formation
Neoproterozoic
Ediacaran
630 Ma
Cryogenian
Marinoan
Sturtian
Torrensian
Umberatana Group
Yerelina Subgroup
Upalinna Subgroup
Nepouie Subgroup
Yudnamutana Subgroup
Reynella Siltstone Member
Whyalla Sandstone
Elatina Formation
Unnamed diamictite member
Balparana Sst
Mount Curtis Tillite
Unnamed sandstone member
Elatina Formation
Fortress Hill Fm
Wilmington Formation equivalent
Wilmington Formation
Marino Arkose member
Yaltipena Fm.
Trezona Fm.
Enorama Shale
Artipena Dolomite member
Wundowie Limestone member
Unnamed sandy limestone member
Amberoona Formation
Trezona Fm.
Enorama Shale
Wundowie Limestone member
Angepena Formation equivalent
Unnamed dolomite member
Angepena Formation
Unnamed dolomite member
Unnamed dolomite member
Unnamed sandstone member
Etina Formation
Sunderland Formation
Cox Sandstone Mbr equivalent
Unnamed limestone member
Yankaninna Fm.
Weetootla Dolomite member
Angepena Formation
Unnamed dolomite member
Brighton Limestone
Tapley Hill Formation
Woocalla Dolomite Member
Tindelpina Shale Member
643 ± 2.4 Ma[1]
Eudunda Arkose Member
Wockerawirra Dolomite Member
Mount Caernarvon Greywacke Member
Balcanoona Formation
Willigan Member
659 ± 6 Ma[2]
Serle Conglomerate
Wilyerpa Fm
Marcowie Dolomite Mbr
Holowilena Ironstone
Lyndhurst Formation
?
Appila Tillite
(MMDD-1 borehole)
Sturt Tillite
Pualco Tillite
Bolla Bollana Tillite
Merinjina Tillite
Belair Subgroup
Lower and middle Burra Group
Callanna Group + pre-Adelaidian rocks
LEGEND
Hiatus
Marinoan glacigenic deposits
Sturtian post-glacial deposits
Sturtian glacigenic deposits
NOTES
†Gradstein et al. (2004)
[1]Re-Os date: basal Tindelpina Shale Mbr (Kendall et al., 2006)
[2]U-Pb date: top Wilyerpa Fm (Fanning & Link, 2006)

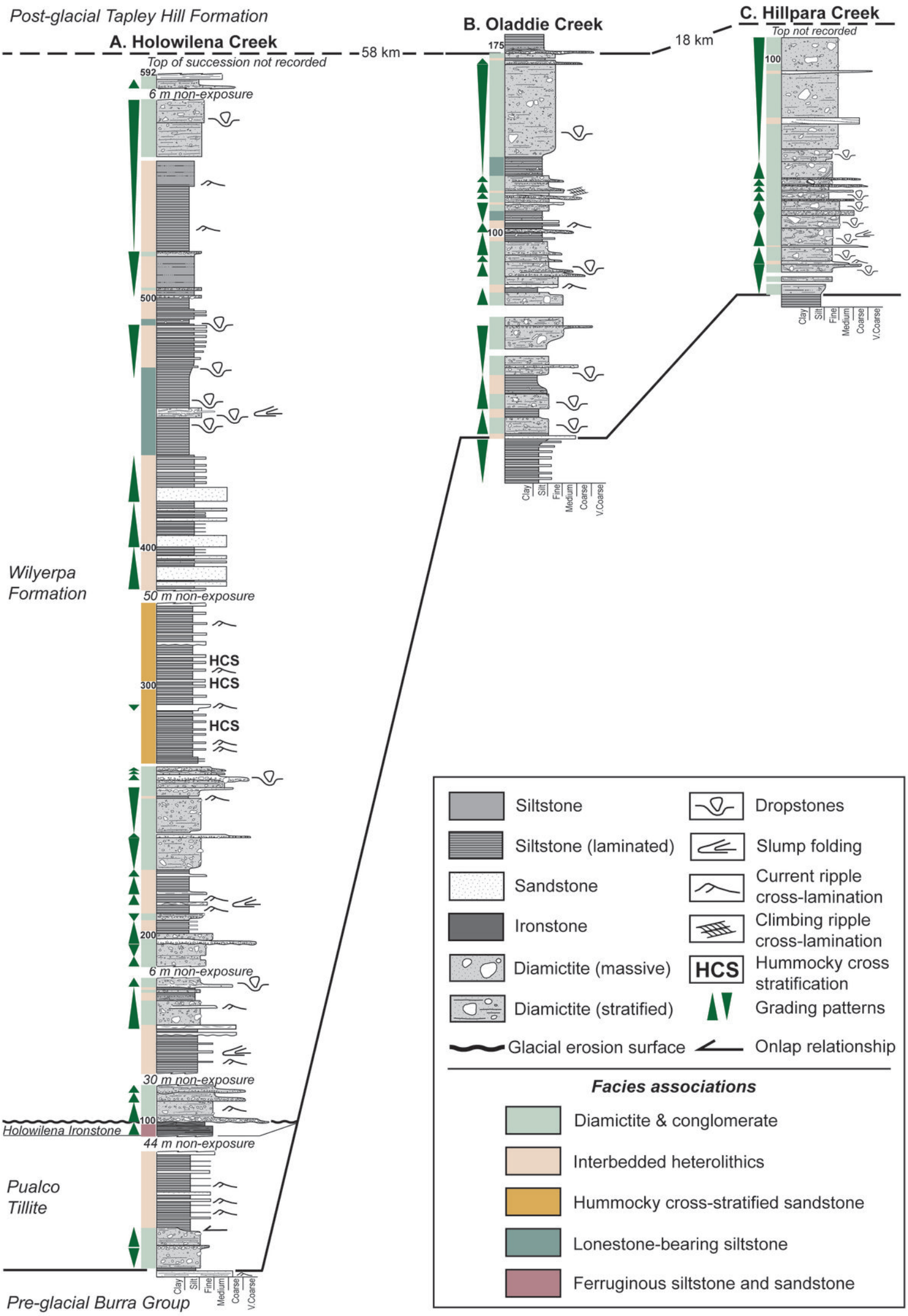
Post-glacial Tapley Hill Formation
A. Holowilena Creek
58 km
B. Oladdie Creek
18 km
C. Hillpara Creek
Top not recorded
Top of succession not recorded
592
6 m non-exposure
500
400
Wilyerpa Formation
50 m non-exposure
HCS
HCS
HCS
300
200
6 m non-exposure
30 m non-exposure
100
Holowilena Ironstone
44 m non-exposure
Pualco Tillite
Pre-glacial Burra Group
175
100
100
Clay
Silt
Fine
Medium
Coarse
V.Coarse
Siltstone
Siltstone (laminated)
Sandstone
Ironstone
Diamictite (massive)
Diamictite (stratified)
Glacial erosion surface
Dropstones
Slump folding
Current ripple cross-lamination
Climbing ripple cross-lamination
HCS
Hummocky cross stratification
Grading patterns
Onlap relationship
Facies associations
Diamictite & conglomerate
Interbedded heterolithics
Hummocky cross-stratified sandstone
Lonestone-bearing siltstone
Ferruginous siltstone and sandstone

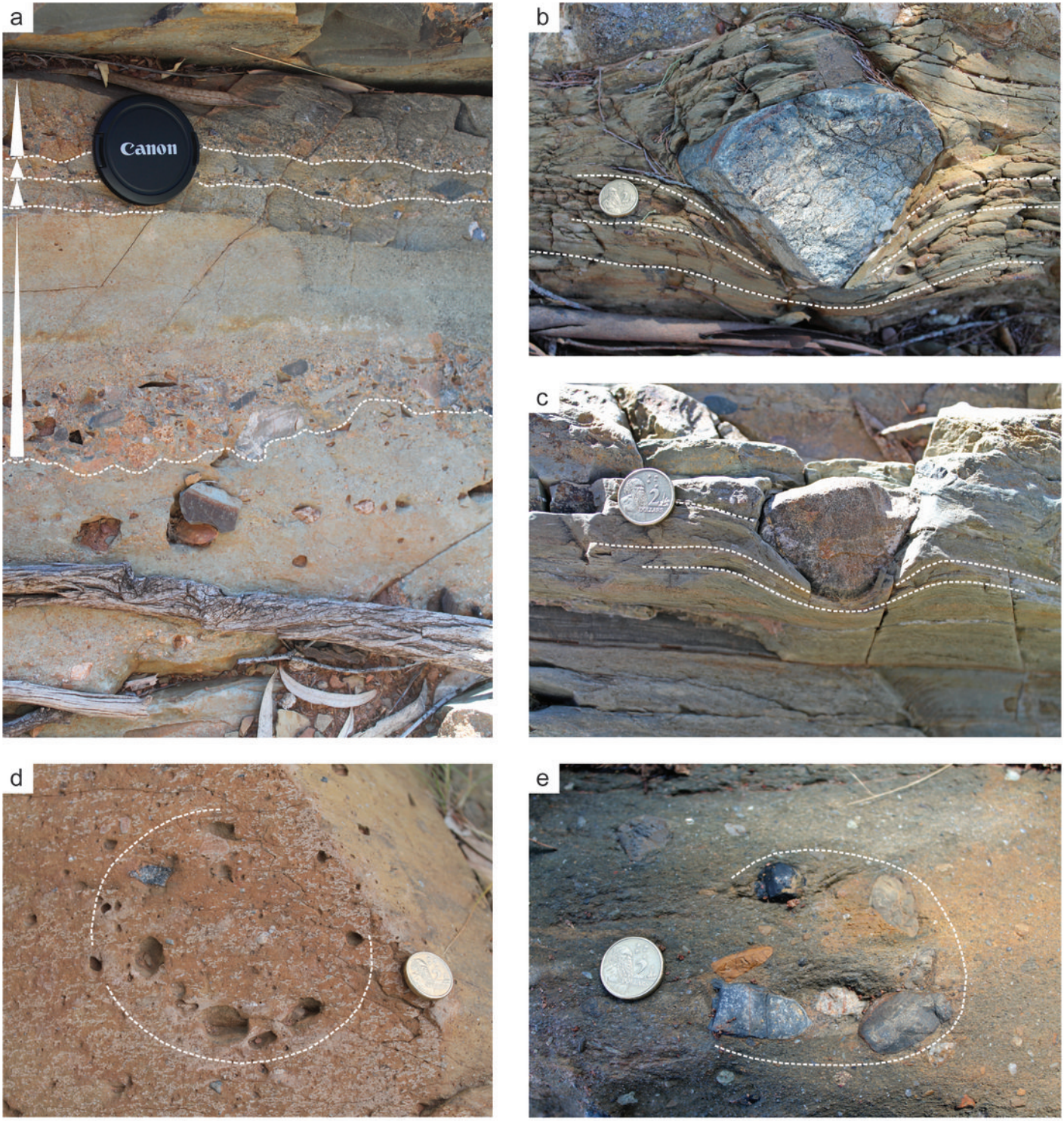
a
Canon
b
c
d
e

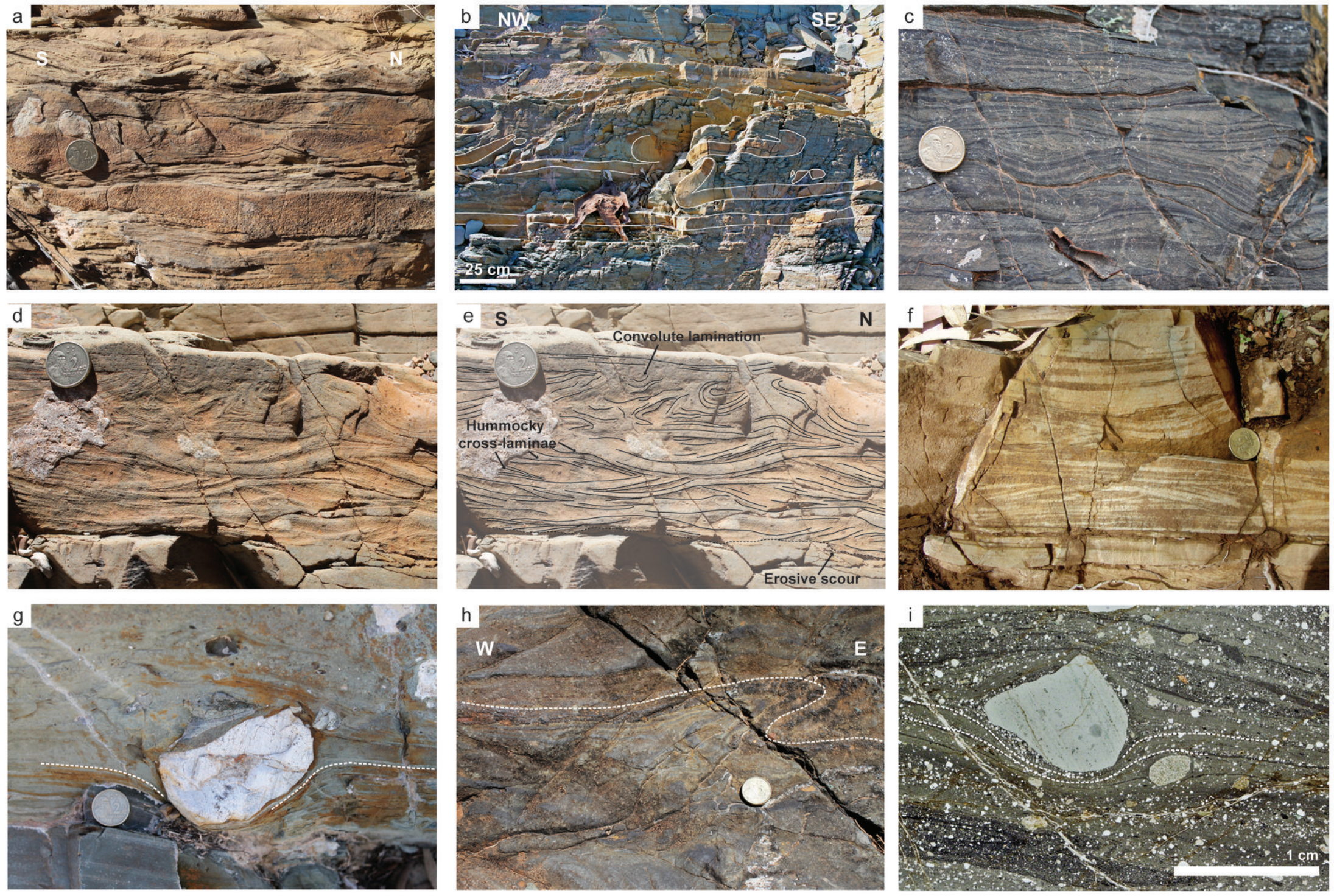
a
S
N
b
NW
SE
25 cm
c
d
e
S
N
Convolute lamination
Hummocky
cross-laminae
Erosive scour
f
g
h
W
E
i
1 cm

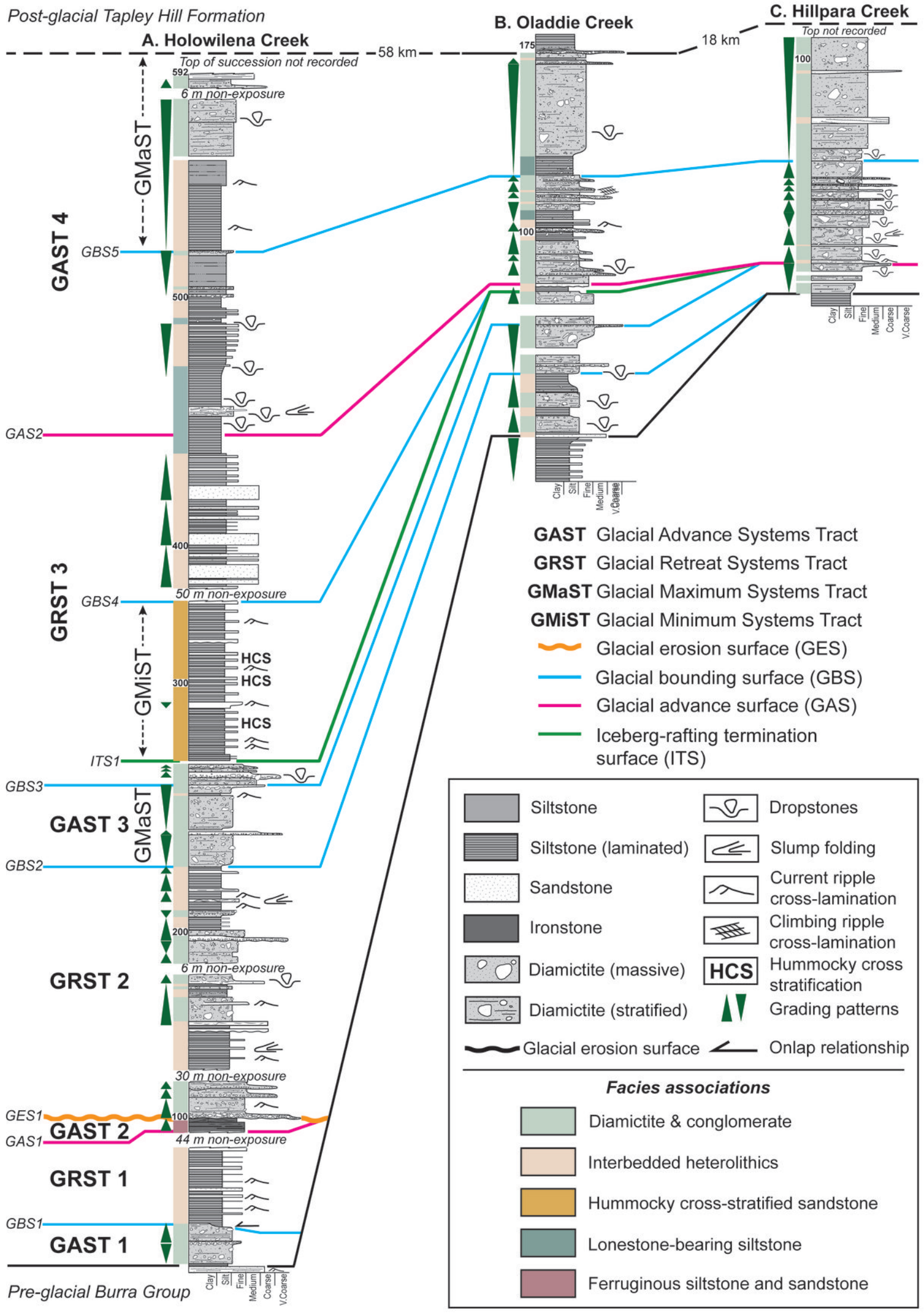
Post-glacial Tapley Hill Formation
A. Holowilena Creek
58 km
B. Oladdie Creek
18 km
C. Hillpara Creek
Top of succession not recorded
Top not recorded
592
175
100
500
400
300
200
100
6 m non-exposure
50 m non-exposure
6 m non-exposure
30 m non-exposure
44 m non-exposure
GMaST
GMiST
GMaST
GMaST
GAST 4
GRST 3
GAST 3
GRST 2
GAST 2
GRST 1
GAST 1
GBS5
GAS2
GBS4
ITS1
GBS3
GBS2
GES1
GAS1
GBS1
HCS
HCS
HCS
Clay
Silt
Fine
Medium
Coarse
V.Coarse
Pre-glacial Burra Group
GAST Glacial Advance Systems Tract
GRST Glacial Retreat Systems Tract
GMaST Glacial Maximum Systems Tract
GMiST Glacial Minimum Systems Tract
Glacial erosion surface (GES)
Glacial bounding surface (GBS)
Glacial advance surface (GAS)
Iceberg-rafting termination surface (ITS)
Siltstone
Siltstone (laminated)
Sandstone
Ironstone
Diamictite (massive)
Diamictite (stratified)
Glacial erosion surface
Dropstones
Slump folding
Current ripple cross-lamination
Climbing ripple cross-lamination
HCS
Hummocky cross stratification
Grading patterns
Onlap relationship
Facies associations
Diamictite & conglomerate
Interbedded heterolithics
Hummocky cross-stratified sandstone
Lonestone-bearing siltstone
Ferruginous siltstone and sandstone

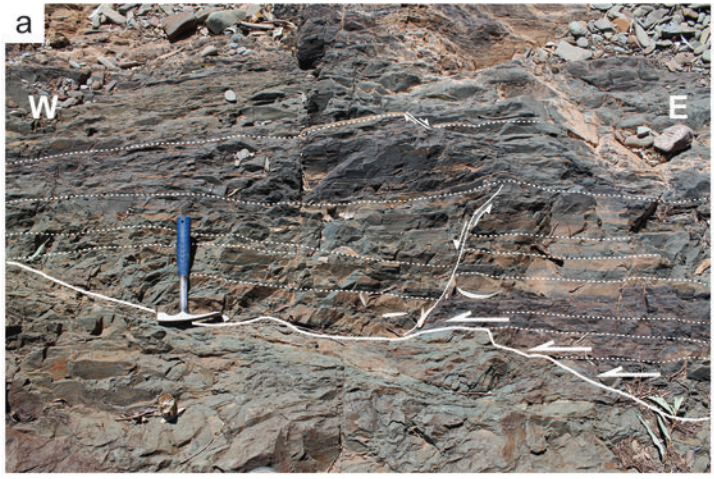
a
W
E


b


c


d
Post-glacial
Tapley Hill Fm.
Terminal
transgressive lag
Glacially-influenced
Wilyerpa Fm.
Canon

N

S

Ice-rafted debris

GMaST
GAST
GRST
GMiST
GRST
GMaST
GRST
GAST
GRST
GAST

Holowilena Creek

Oladdie Creek

Hillpara Station

Glaciogenic debris flows
and turbidites

c. 65 km

Sequence boundaries

Glacial bounding surface (GBS)

Glacial erosion surface (GES)

Glacial advance surface (GAS)

Iceberg-rafting termination surface (ITS)

Facies associations

Diamictite & conglomerate

Interbedded heterolithics

Hummocky cross-stratified sandstone

Lonestone-bearing siltstone

Ferruginous siltstone and sandstone